

Full Research Paper

Sensor Performance Requirements for the Retrieval of Atmospheric Aerosols by Airborne Optical Remote Sensing

Felix Seidel^{1,*}, **Daniel Schläpfer**¹, **Jens Nieke**² and **Klaus I. Itten**¹

¹ University of Zürich, Remote Sensing Laboratories, Zürich, Switzerland

E-mail: felix.seidel@geo.uzh.ch, daniel@rese.ch, klaus.itten@geo.uzh.ch.

² ESA / ESTEC, Noordwijk, Netherlands

E-mail: jens.nieke@esa.int.

* Author to whom correspondence should be addressed.

Received: 30 January 2008 / Accepted: 17 March 2008 / Published: 18 March 2008

Abstract: This study explores performance requirements for the retrieval of the atmospheric aerosol optical depth (AOD) by airborne optical remote sensing instruments. Independent of any retrieval techniques, the calculated AOD retrieval requirements are compared with the expected performance parameters of the upcoming hyperspectral sensor APEX at the reference wavelength of 550nm. The AOD accuracy requirements are defined to be capable of resolving transmittance differences of 0.01 to 0.04 according to the demands of atmospheric corrections for remote sensing applications. For the purposes of this analysis, the signal at the sensor level is simulated by radiation transfer equations. The resulting radiances are translated into the AOD retrieval sensitivity ($\Delta\tau_{\lambda}^{aer}$) and compared to the available measuring sensitivity of the sensor ($NE\Delta L_{\lambda}^{sensor}$). This is done for multiple signal-to-noise ratios (SNR) and surface reflectance values. It is shown that an SNR of 100 is adequate for AOD retrieval at 550nm under typical remote sensing conditions and a surface reflectance of 10% or less. Such dark surfaces require the lowest SNR values and therefore offer the best sensitivity for measuring AOD. Brighter surfaces with up to 30% reflectance require an SNR of around 300. It is shown that AOD retrieval for targets above 50% surface reflectance is more problematic with the current sensor performance as it may require an SNR larger than 1000. In general, feasibility is proven for the analyzed cases under simulated conditions.

Keywords: Aerosol retrieval, SNR, AOD, Radiative transfer, APEX.

1. Introduction

It is known that atmospheric aerosols influence the Earth climate system. Various efforts are being made to investigate the global distribution and concentration of these aerosols and to quantify their forcing on the radiation budget. Numerous data from passive optical Earth observation satellites are used to map aerosol properties on a global scale. Not only atmospheric scientists, but also the remote sensing community relies on aerosol information. Earth observation data in particular have to be corrected for the atmospheric influence in order to provide accurate physical measuring quantities.

During the last two decades, several aerosol retrieval techniques have been developed for satellite instruments. An overview is given by [1] and recent inter-comparisons are provided for the retrieval over land by [2] and over sea by [3], [4] and [5]. In general, relatively large discrepancies between different satellite instruments were found, especially on the scale of single pixels [2]. Even long-term studies over the ocean reveal differences between well established satellite instruments of up to 0.1 aerosol optical depth (AOD or τ_{λ}^{aer}) and 0.45 Ångström exponent [4].

State-of-the-art hyperspectral airborne imagers may be able to outperform the limitations of most current satellite instruments. For example, the typical ground sampling distance (GSD) of spaceborne instruments retrieving AOD routinely is in the range of $1km$ to $30km$. The resulting uncertainty of the surface reflectance is an important contribution to the inaccuracy of the retrieved AOD over land. On the other hand, the GSD of airborne instruments is in the range of meters. One can therefore assume better performances in AOD retrieval over land because the unmixing of the surface and the atmospheric signal is expected to be less difficult. The increased likelihood of observing a uniform surface within one pixel leads to smaller uncertainties in the assumptions about the surface reflectance. This is a major source of error in most satellite-based AOD retrievals. In addition, the use of a hyperspectral sensor allows the avoidance of atmosphere gaseous absorption bands and the use of the complete spectrum from near-UV to SWIR if desired. Furthermore, the spectral and the spatial domain can be binned (adding bands or pixels together) to achieve the desired signal-to-noise ratio (SNR). The Airborne Prism EXperiment (APEX) [6] is chosen for this paper as an example for such an airborne hyperspectral instrument.

This study assesses the feasibility of aerosol retrieval with APEX in terms of the SNR and independent of any particular AOD retrieval technique, which was previously proposed by [7] and [8]. A model which translates atmospheric conditions and surface reflectance into radiance values at-sensor is essential for the establishment of feasibility. It needs also to address the multiple scattering of light while being as simple as possible to avoid excessive computational time or alternatively the use of precalculated look-up tables. This study analyses the SNR requirements and limitations of aerosol retrieval with a focus on the influence of the surface reflectance.

All calculations are carried out at the commonly used aerosol reference wavelength of $550nm$ to make the results comparable to other studies. Preliminary analysis at other wavelengths within the visible spectrum did not reveal qualitative differences to the findings at $550nm$ and are therefore not shown in this paper. The figures are plotted for $0 < \tau_{550nm}^{aer} < 1$ on the x-axis because the minimum expected visibility for an airborne remote sensing campaign will be about $5km$ ($\tau_{550nm}^{aer} \approx 1$). Flights usually will be carried out at visibilities of more than $10km$ ($\tau_{550nm}^{aer} \approx 0.6$).

2. Sensor Characteristics of APEX

APEX is a dispersive push-broom imaging spectrometer, which is expected to provide unique hyperspectral data to geophysical and biochemical studies on land, water and atmospheric processes. APEX will contribute to the Earth observation community by simulating, calibrating and validating future space- and airborne optical sensors. The expected performance of APEX along with a novel spectral, radiometric and geometric calibration methodology provide an opportunity to overcome limitations of currently available remote sensing instruments. This potential is especially important in addressing the requirements for the remote sensing of aerosols.

APEX features more than 500 spectral bands from 385nm to 2500nm with a sampling interval of 0.4nm to 10nm in the full spectral mode. The standard spectral mode comprises more than 300 bands, where bands are binned together to increase the SNR. The typical gain in SNR is in the order of 40% per domain (spectral or spatial). This corresponds to a factor of $1.4^2 \approx 2$ for the binning in both domains.

The GSD is governed by 0.028° instantaneous field of view and 1000 pixels across track. It varies from 2.5m to 8m depending on the flight altitude.

Table 1 provides the preflight APEX-specific sensor performance for minimum, average and maximum radiance levels at 550nm (L_{550nm}^{sensor}). They correspond to surface reflectances (ρ_{550nm}^{sfc}) of 0%, 30% and 100%. $\rho_{550nm}^{sfc} = 0.3$ represents a relatively bright surface reflectance, which can be expected during remote sensing campaigns over land. The minimum and maximum surface reflectance was chosen to account for the extreme values following [9]. The sensor performance is expressed by the noise equivalent spectral radiance difference ($NE \Delta L_{550nm}^{sensor}$). The relation between L_{550nm}^{sensor} and $NE \Delta L_{550nm}^{sensor}$ is given by:

$$NE \Delta L_{\lambda}^{sensor} = \frac{L_{\lambda}^{sensor}}{SNR_{\lambda}}, \quad (1)$$

where SNR_{λ} is the band-specific signal-to-noise ratio or sensor efficiency. It consists of the instrument and photon noise. The latter is mainly a function of the spectral radiance level L_{λ}^{sensor} .

The actual sensor performance values are going to be measured in mid 2008 during the first full calibration of APEX. This instrument is currently in assembly and its maiden flight is scheduled later in 2008.

Table 1. Preflight values at 550nm for the spectral radiance resolvability of APEX ($NE \Delta L_{550nm}^{sensor}$) for the corresponding minimum ($\rho_{550nm}^{sfc} = 0.0$), average ($\rho_{550nm}^{sfc} = 0.3$) and maximum ($\rho_{550nm}^{sfc} = 1.0$) spectral radiance level at the sensor (L_{550nm}^{sensor}). The values are given in units of [$W \cdot m^{-2} \cdot sr^{-1} \cdot nm^{-1}$] and based on the APEX standard spectral binning pattern.

Minimum		Average		Maximum	
L_{550nm}^{sensor}	$NE \Delta L_{550nm}^{sensor}$	L_{550nm}^{sensor}	$NE \Delta L_{550nm}^{sensor}$	L_{550nm}^{sensor}	$NE \Delta L_{550nm}^{sensor}$
0.01631	0.00019	0.09762	0.00030	0.51699	0.00060

3. Radiance Simulation

Some basic radiation transfer equations are needed to simulate the attenuation of the light traveling from the top of the atmosphere down to a surface pixel and upward to the airborne sensor. The upwelling spectral radiance into an instrument (at-sensor-radiance L_{λ}^{sensor}) is a function of successive orders of radiation interactions within the coupled surface-atmosphere system. In theory, it can be decoupled into a contribution from the atmosphere (path-radiance L_{λ}^{atm}) and from the underlying surface (L_{λ}^{sfc}). L_{λ}^{atm} can be split into the direct ($L_{\lambda}^{atm,drc}$) and the diffuse ($L_{\lambda}^{atm,dfs}$) reflected spectral radiance from the scattering atmospheric layer:

$$L_{\lambda}^{sensor} = L_{\lambda}^{atm} + L_{\lambda}^{sfc} = L_{\lambda}^{atm,drc} + L_{\lambda}^{atm,dfs} + L_{\lambda}^{sfc} \quad (2)$$

3.1. Path-Radiance

If we assume a homogeneous scattering layer and the single scattering approximation (SSA), the atmospheric spectral path-radiance can be derived from the well known Radiation Transfer Equation by [10] as follows:

$$L_{\lambda,SSA}^{atm} = \underbrace{\frac{E_{0\lambda}\mu_0}{\pi}}_I \underbrace{\left[1 - e^{-\tau_{\lambda}\left(\frac{1}{\mu_0} + \frac{1}{\mu}\right)}\right]}_{II} \underbrace{\frac{\omega_0 P_{\lambda}(\Theta)}{4(\mu + \mu_0)}}_{III}, \quad (3)$$

where the incoming spectral radiance (I) is reflected by the scattering atmosphere (II) and scattered directly (single scattering) into the sensor's viewing geometry (III). $E_{0\lambda}\mu_0$ is the solar spectral irradiance, scaled by the cosine of the solar zenith angle. μ describes the sensor viewing geometry, where $\mu = \cos(0^\circ) = 1$ is valid for a nadir viewing instrument, such as APEX. The atmospheric single scattering albedo ω_0 is the ratio of the scattering to the extinction coefficient. The atmospheric phase function $P_{\lambda}(\Theta)$ takes care of the amount of light, which is diverted into the sensor viewing direction. For aerosol remote sensing, the atmospheric optical depth can be decomposed into its molecular and particle (aerosol) extinction part, such that $\tau_{\lambda} = \tau_{\lambda}^{mlc} + \tau_{\lambda}^{aer}$.

The multiple scattering of light at molecules and aerosols is an important contribution to L_{λ}^{sensor} for $\lambda < 800nm$. It leads to increasing errors for smaller λ due to the SSA in Equation 3. Unfortunately, multiple scattering is difficult to express in form of a simple equation. But its influence can be taken into account by introducing a correction factor $f(\tau_{\lambda})$ [11]:

$$f(\tau_{\lambda}) = \frac{L_{\lambda}^{atm}}{L_{\lambda,SSA}^{atm}}. \quad (4)$$

It represents the ratio of the exact radiance calculation by a multiple scattering radiation transfer code (i.e. [12] or [11]) to the SSA radiance calculation. $f(\tau_{\lambda})$ can be interpreted in Figure 1(a) by taking the ratio between the MODTRAN4 [13] curve and the SSA curve from Equation 3. One finds that the multiple scattering intensifies L_{λ}^{sensor} by a factor of 1.5 at $\tau_{550nm}^{aer} = 0.2$ and by a factor of 2.0 at $\tau_{550nm}^{aer} = 0.85$.

The atmospheric spectral radiance corrected for the multiple scattered light is therefore given by:

$$L_{\lambda}^{atm} = \frac{E_{0\lambda}\mu_0}{\pi} \left[1 - e^{-\tau_{\lambda}\left(\frac{1}{\mu_0} + \frac{1}{\mu}\right)}\right] \frac{\omega_0 P_{\lambda}(\Theta)}{4(\mu + \mu_0)} f(\tau_{\lambda}). \quad (5)$$

3.2. Surface Contribution

Since L_{λ}^{sfc} is often the dominating contribution to L_{λ}^{sensor} , one must account for the underlying surface. The ratio of incoming and outgoing spectral irradiance at the surface level yields the homogeneous Lambertian surface reflectance: $E_{\lambda}^{\downarrow sfc}/E_{\lambda}^{\uparrow sfc} = \rho_{\lambda}^{sfc}$. Since $E_{\lambda}^{\uparrow sfc} \equiv \pi L_{\lambda}^{sfc}$ and therefore $E_{\lambda}^{\downarrow sfc}/\pi\rho_{\lambda}^{sfc} = L_{\lambda}^{sfc}$ we find:

$$L_{\lambda}^{sfc} = \frac{E_{0\lambda}\mu_0}{\pi} \frac{\rho_{\lambda}^{sfc}T_{\lambda}^{\uparrow}}{1 - s_{\lambda}\rho_{\lambda}^{sfc}}. \quad (6)$$

s_{λ} is the spherical albedo and describes the portion of the light scattered back to the surface as a result of isotropic illumination of the atmosphere by the surface. It is therefore also a function of T_{λ} and τ_{λ} . T_{λ}^{\uparrow} denotes the total spectral transmittance, comprising of the down- and upward direct ($T_{\lambda}^{\downarrow drc, sca}$) and diffuse ($T_{\lambda}^{\downarrow dfs, sca}$) scattering transmittance and the absorption transmittance (T_{λ}^{abs}):

$$T_{\lambda}^{\uparrow} = \left(T_{\lambda}^{\downarrow drc, sca} + T_{\lambda}^{\downarrow dfs, sca}\right) T_{\lambda}^{\downarrow abs} \left(T_{\lambda}^{\uparrow drc, sca} + T_{\lambda}^{\uparrow dfs, sca}\right) T_{\lambda}^{\uparrow abs}. \quad (7)$$

[14] offers a parameterization by polynomial series with a satisfying accuracy to describe $T_{\lambda}^{\downarrow dfs, sca}$ and s_{λ} . Additionally, a non-uniform surface could be considered by adjusting ρ_{λ}^{sfc} in the denominator of Equation 6 to incorporate an environment reflectance according to [15] and [16] or [17].

3.3. At-Sensor-Radiance

In the case of an airborne remote sensor, the atmospheric extinction has to be adjusted to the reduced atmospheric path length between the surface and the sensor. An approximating method would be to use the air pressure ratio (p^*) between the sensor and the surface level to scale the upward optical depth due to molecular scattering: $p^* \cdot \tau_{\lambda}^{\uparrow mlc}$, which is equal to $(T_{\lambda}^{\uparrow mlc})^{p^*}$. The extinction by aerosols above the sensor (ie. background volcanic particles in the stratosphere) is neglected here. For this study, p^* is set to 0.5, which corresponds to a sensor height of about 5500 meters above sea level using the international standard atmosphere.

Finally, the complete spectral radiance at the sensor level is given by adding Equations 5 and 6:

$$L_{\lambda}^{sensor} = \frac{E_{0\lambda}\mu_0}{\pi} \left[\left[1 - e^{-\tau_{\lambda}\left(\frac{1}{\mu_0} + \frac{1}{\mu}\right)} \right] \frac{\omega_0 P_{\lambda}(\Theta)}{4(\mu + \mu_0)} f(\tau_{\lambda}) + \frac{\rho_{\lambda}^{sfc} T_{\lambda}^{\uparrow}}{1 - s_{\lambda}\rho_{\lambda}^{sfc}} \right]. \quad (8)$$

3.4. Verification with MODTRAN4

Equation 8 was compared against results from the widely accepted radiation transfer model MODTRAN4 [13] including the multiple stream algorithm DISORT [12] to account for the multiple scattering. The 1976 U.S. Standard Model Atmosphere was used to describe the vertical profile of gas mixing ratios. The aerosol optical properties within the planetary boundary layer were taken into account in MODTRAN4 by a rural type of aerosol with a mixing ratio of 0.7 small water-soluble and 0.3 large

Table 2. Variables used in Equation 8 to plot the figures of this paper . τ_{λ}^{mlc} is tabulated in [19].

Variables independent of τ_{550nm}^{aer} :	μ_0	μ	$\Theta_{\mu_0,\mu}$ [°]	$E_{0;550nm}$ [$W \cdot m^{-2} \cdot nm^{-1}$]	τ_{550nm}^{mlc}
	0.733	1.00	137	1.90	0.097

Variables depending on τ_{550nm}^{aer} :	ω_0	P_{550nm} (Θ)	s_{550nm}
$\tau_{550nm}^{aer} = 0.05$	0.99	0.90	0.10
$\tau_{550nm}^{aer} = 0.5$	0.97	0.87	0.20

dust-like particles. A tropospheric type with small water soluble particles was used for the free troposphere. Equation 8 was fed by the Average Continental model from [18], which adds a few particles of soot (0.06 mixing ratio) to the troposphere type. The results and conclusions of this paper were derived by means of Equation 8 and they are therefore not affected by differences in the aerosol models. Further parameters used with Equation 8 and with MODTRAN4 for the verification are given in Table 2.

Figure 1 presents the simulation of L_{λ}^{sensor} as a function of τ_{λ}^{aer} . The black lines are the results from Equation 8 over different ρ_{λ}^{sfc} while the colored lines with circles referring to the MODTRAN4 reference

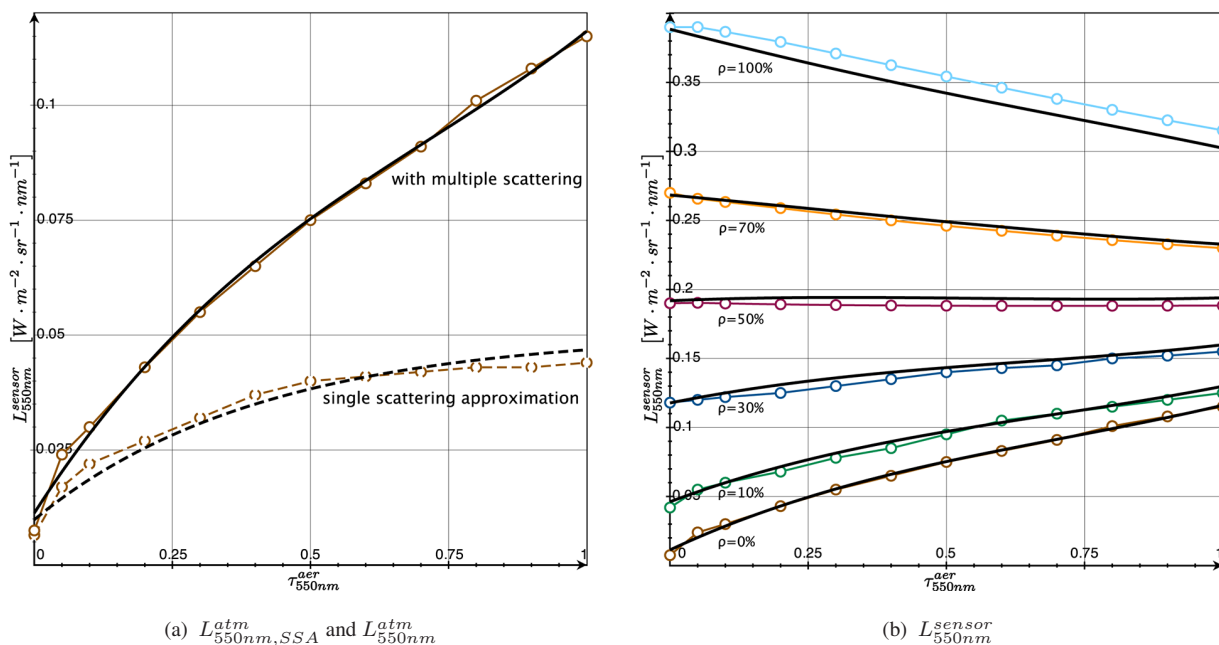


Figure 1. Black lines show the radiance simulations, while the MODTRAN4 reference calculations are given by colored lines with circles. (a) Influence of AOD (τ_{550nm}^{aer}) on the observed path-radiance ($\rho_{\lambda}^{sfc}=0$) with the single scattering approximation ($L_{550nm,SSA}^{atm}$) from Equation 3 and with multiple scattering (L_{550nm}^{atm}) from Equation 5. (b) Influence of τ_{550nm}^{aer} on the observed radiance (L_{550nm}^{sensor}) including the surface contribution from Equation (8). $\rho = ..\%$ denotes the corresponding surface reflectance ρ_{λ}^{sfc} .

calculations. Figure 1(a) shows the intermediate step with the SSA (dashed lines) over a black surface ($\rho_{550nm}^{sfc} = 0$), which is given by Equation 3. The influence of the multiple scattering is clearly visible as the offset between the dashed and the solid line. This offset is represented in the multiple scattering correction factor $f(\tau_\lambda)$ used in Equation 5.

The accuracy of the spectral radiance simulation is given by qualitatively comparing the results for $L_{550nm,SSA}^{atm}$ and L_{550nm}^{atm} with the MODTRAN4 reference calculations in Figure 1(a). The effect of the surface contribution by Equation 6 can be seen in Figure 1(b), where the complete L_λ^{sensor} from Equation 8 is given for different surface reflectances along with the MODTRAN4 results.

At $\rho_\lambda^{sfc} \cong 0.5$, the model expects to cancel out the change in absorption and the change in scattering due to a changing AOD. L_λ^{sensor} is therefore no longer a function of τ_λ^{aer} , which makes it impossible to retrieve AOD at a surface reflectance of about 50%. Further investigations showed that this critical ρ_λ^{sfc} varies with the aerosol scattering properties ω_0 , $P_\lambda(\Theta)$ and with μ_0 , μ and s_λ (not shown).

4. Sensitivity Requirements

4.1. AOD Retrieval Sensitivity Requirements

The atmosphere has a distorting effect on L_λ^{sensor} , which has to be compensated for quantitative remote sensing applications. AOD is a crucial parameter for the atmospheric correction process to derive accurate apparent surface reflectances. We define an accuracy requirement of 1% absolute error in surface reflectance according to [20]. This can be also expressed in terms of transmittance in order to relate it to AOD. A rough estimation of the allowed application specific error (ε) in $T_{550nm}^{\uparrow drc, sca} = e^{-\tau_{550nm}}$ yields 0.01 transmittance values for dark surfaces, such as water bodies ($\rho_{550nm}^{sfc} \approx 0.05$). The relative influence of L_λ^{atm} on L_λ^{sensor} is decreasing for increasing ρ_λ^{sfc} (Equation 8). For example, at $\rho_{550nm}^{sfc} = 0.3$ the L_{550nm}^{atm} accounts for about 25% of L_{550nm}^{sensor} at $\tau_{550nm}^{aer} = 0.1$ (see Figure 1(b)) and therefore ε yields 0.04 transmittance values.

The required retrieval sensitivity of the total optical depth is calculated by:

$$\Delta\tau_\lambda = \frac{\varepsilon}{\left| \frac{d}{d\tau_\lambda} T_\lambda^{\uparrow drc, sca} \right|} = |-\varepsilon e^{\tau_\lambda}|. \quad (9)$$

The exponential dependence of $\Delta\tau_\lambda$ on the total optical depth and therefore also on AOD is obvious. It is found that $\Delta\tau_\lambda^{aer} \leq 0.01$ is needed for the worst case of a dark surface and low AOD conditions ($\tau_\lambda^{aer} \rightarrow 0$). A $\Delta\tau_\lambda^{aer} \leq 0.045$ is satisfactory for $\rho_{550nm}^{sfc} \approx 0.3$. Equation 9 is also used later in Figures 2 and 3 to define AOD retrieval requirements.

4.2. Sensor Sensitivity Requirements

The results from AOD retrieval sensitivity requirements can now be used to define the performance requirements of an optical remote sensing instrument because they are related to the radiometric resolvability (ΔL_λ). This is a prerequisite for the successful retrieval of aerosols. For obvious reason, the radiance variation induced due to change in AOD must exceed $NE \Delta L_\lambda$ of a sensor [21]:

$$\Delta\tau_\lambda^{aer} \propto \Delta L_\lambda^{aer} \geq NE \Delta L_\lambda^{sensor}. \quad (10)$$

The sensor-specific sensitivity on AOD ($NE \Delta\tau_\lambda^{aer}$) is given by means of the simulated L_λ^{sensor} from Equation 8 and $NE \Delta L_\lambda^{sensor}$ from Equations 1 and 10:

$$NE \Delta\tau_\lambda^{aer} = \frac{1}{\frac{d}{d\tau_\lambda^{aer}} L_\lambda^{sensor}} NE \Delta L_\lambda^{sensor}. \quad (11)$$

5. Results

5.1. SNR Requirements

Figure 2 assesses the SNR requirements depending on surface reflectance and AOD. The retrieval of τ_λ^{aer} is feasible as long as $NE \Delta\tau_\lambda^{aer} \leq \tau_\lambda^{aer}$ according to Equation 10. The area where this limit is not fulfilled, because the noise exceeds the signal, is drawn in dark-red in Figures 2 and 3. The dark orange color denotes the area where the desired minimal aerosol retrieval interval ($\Delta\tau_\lambda^{aer}$) from Equation 9 can not be achieved for the $\varepsilon = 0.04$ requirement. The stricter $\varepsilon = 0.01$ is met within the white area.

Over dark surfaces, where L_λ^{atm} dominates L_λ^{sensor} , AOD retrieval sensitivity is best for small AOD. This is because small $NE \Delta\tau_\lambda^{aer}$ can be achieved even for relative low SNR values (Figures 2(a) and 2(b)). An SNR of less than 100 is enough to fulfill the strict atmospheric correction accuracy requirement of $\varepsilon = 0.01$, which is needed for dark targets. Assuming a typical case with a surface of $\rho_{550nm}^{sfc} = 0.1$ and $\tau_{550nm}^{aer} = 0.15 \pm 0.1$, a $NE \Delta\tau_\lambda^{aer}$ of at least 0.008 for $SNR = 100$ can be expected.

Brighter surfaces ($0.1 < \rho_{550nm}^{sfc} < 0.3$) require greater SNR to keep a certain aerosol retrieval sensitivity compared to dark surfaces. This range of surface reflectances is expected to be the typical case for remote sensing over land. To fulfill $\varepsilon = 0.01$, an SNR between 100 and 300 is now required. In terms of atmospheric correction ε can be relaxed to 0.04, where an SNR between 30 and 100 is sufficient (Figures 2(c) and 2(d)). An SNR of 300 allows an aerosol retrieval sensitivity of less than 0.01 with $\tau_{550nm}^{aer} \leq 0.25$, which is expected to be the typical condition for most flight campaigns.

Very bright surfaces ($0.4 < \rho_{550nm}^{sfc} < 0.6$) are found to be most challenging because L_{550nm}^{sensor} depends weakly on τ_{550nm}^{aer} . Changes in scattering and absorption of light due to a $\Delta\tau_\lambda^{aer}$ may cancel each other out. It can be seen in Figure 1(b), Equation 8 and MODTRAN4 reveal virtually no influence of the aerosol loading on L_{550nm}^{sensor} in the case of $\rho_{550nm}^{sfc} \approx 0.5$. Due to the derivation of a local minimum in Equation 11, $NE \Delta\tau_{550nm}^{aer}$ can go to infinity as plotted in Figure 2(e). This critical surface reflectance of about 50% as well as the position (in terms of τ_{550nm}^{aer}) of $NE \Delta\tau_{550nm}^{aer} \rightarrow \infty$ depends on many parameters and can vary between different models. This effect is not analyzed in detail here but shows clearly that aerosol retrieval can be difficult for a certain small range of surface reflectances.

Extremely bright targets, such as snow and clouds, provide adequate sensitivity. Figure 2(f) shows an example for $\rho_{550nm}^{sfc} = 0.8$, where an SNR of about 100 is sufficient for $\varepsilon = 0.04$, while 300 is needed for the $\varepsilon = 0.01$ requirement. The sensitivity is almost constant over the typical range of τ_{550nm}^{aer} at this surface reflectance. This is in contrast to the calculations with low surface reflectance ($\rho_{550nm}^{sfc} < 0.4$), where $NE \Delta\tau_{550nm}^{aer}$ generally decreases for increasing τ_{550nm}^{aer} .

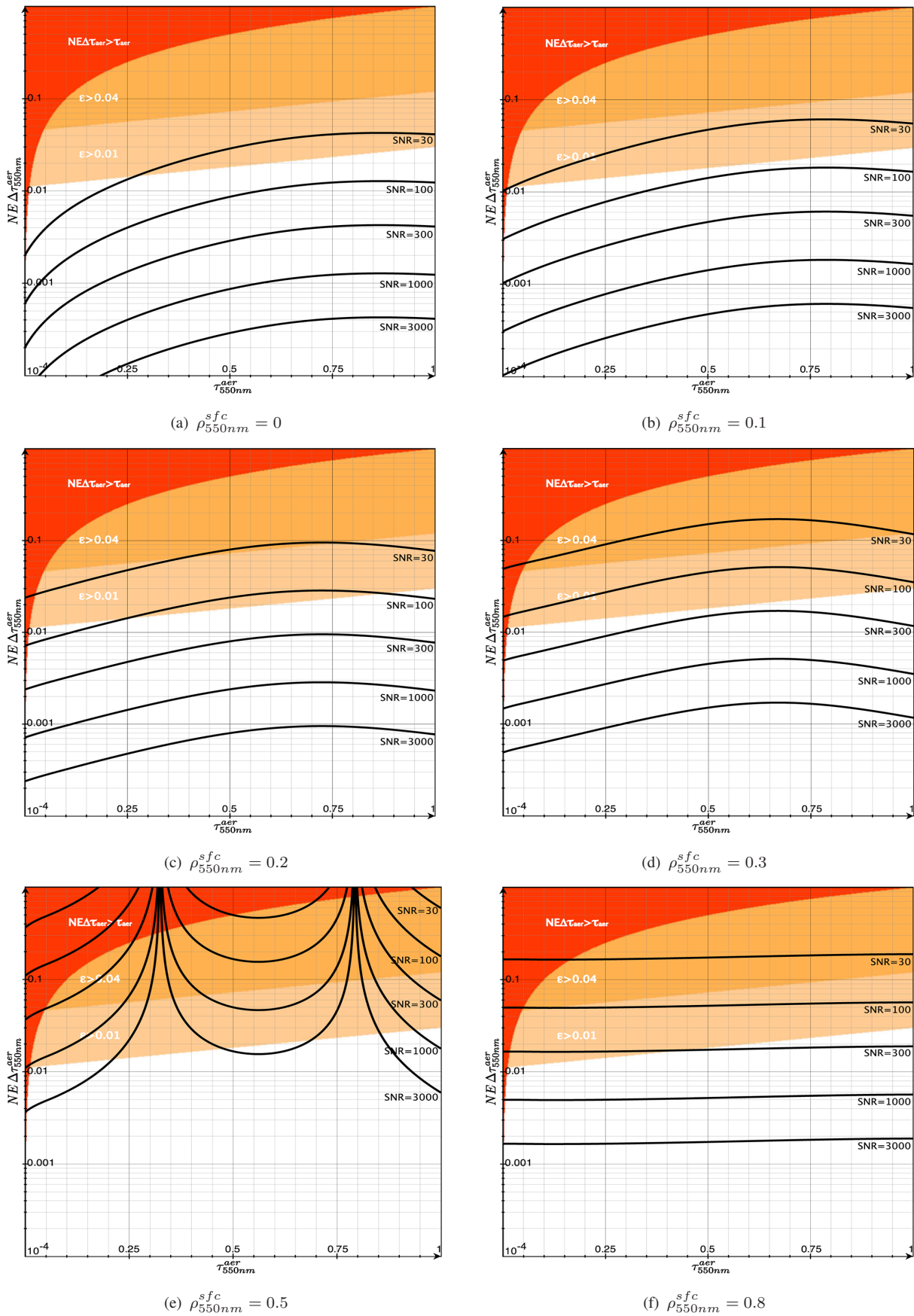


Figure 2. Influence of τ_{550nm}^{aer} on the AOD retrieval sensitivity $NE \Delta \tau_{550nm}^{aer}$ for different SNR values. AOD retrieval is feasible outside the red area, while the transmittance accuracy requirement complies with $0.01 < \varepsilon < 0.04$ within the light orange area and with $\varepsilon < 0.01$ within the white area.

5.2. Influence of the Surface Reflectance

The influence of the surface reflectance on aerosol retrieval is highlighted by Figure 3. 3(a) reveals clearly that an $SNR \geq 100$ is needed to detect aerosols over typical surfaces. Such an SNR allows achieving $\varepsilon = 0.01$ with dark surfaces and $\varepsilon = 0.04$ with $\rho_{550nm}^{sfc} = 0.3$ and 1.0 . $\rho_{550nm}^{sfc} \leq 0.1$ is mostly unproblematic for instruments with SNR greater than 50. A surface reflectance of $\rho_{550nm}^{sfc} \leq 0.4$ or $\rho_{550nm}^{sfc} \geq 0.8$ requires an instrument with an SNR of about 400 to fulfill the strict requirement (Figure 3(b)). It is possible to achieve $\varepsilon = 0.04$ with the same SNR also for $\rho_{550nm}^{sfc} \leq 0.45$ and $\rho_{550nm}^{sfc} \geq 0.6$. Greater SNR enhances the retrieval sensitivity within the white area, where $\varepsilon < 0.01$ is given.

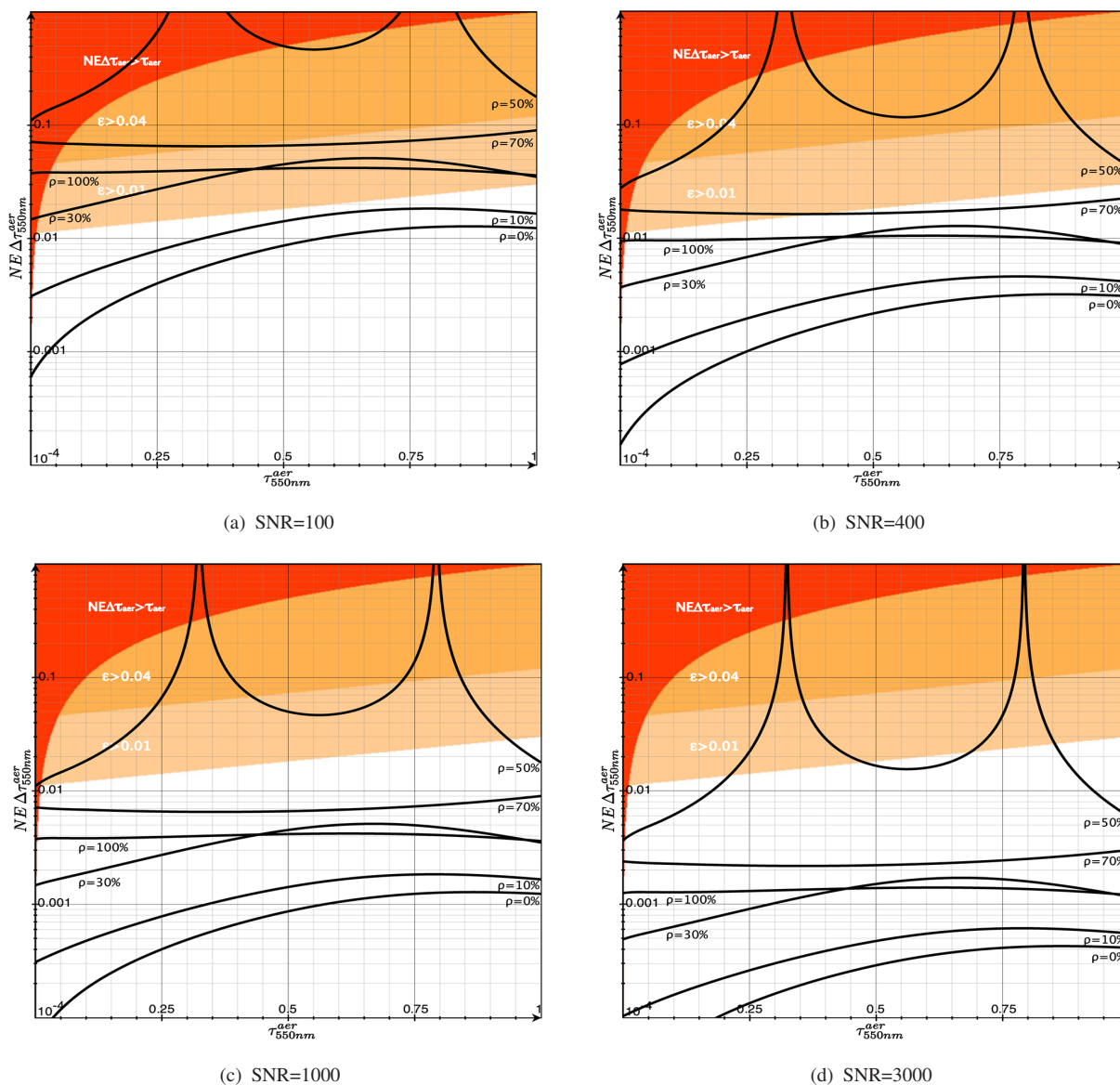


Figure 3. Influence of τ_{550nm}^{aer} on the AOD retrieval sensitivity $NE \Delta \tau_{550nm}^{aer}$ for different surface reflectances ρ_{550nm}^{sfc} . AOD retrieval is feasible outside the red area, while the transmittance accuracy requirement complies with $0.01 < \varepsilon < 0.04$ within the light orange area and with $\varepsilon < 0.01$ within the white area.

Much higher SNR are required in order to detect aerosols over a surface reflectance of around 50%. Figures 3(c) and 3(d) show that the requirement of $\varepsilon = 0.04$ can be met within a range of $\tau_{550nm}^{aer} = \{0.01 - 0.25, 0.45 - 0.7, 0.85 - 1.0\}$ with an SNR of 1000. This AOD range becomes smaller for a larger SNR. $\varepsilon = 0.01$ can only be met partially by having an SNR of more than 3000. This can be achieved only by trading off foremost spatial and/or spectral resolution for SNR by binning hyperspectral remote sensing data in these domains.

5.3. Feasibility of Aerosol Retrieval with APEX

The crucial question is whether an aerosol retrieval is possible with an airborne hyperspectral sensor optical system, such as APEX. It must be demonstrated that the required signal sensitivity is provided by the instrument. Since APEX has not yet undergone a complete calibration process, one must use preflight SNR requirements for this analysis. These values are given in Table 1 with $NE \Delta L_{550nm}^{sensor}$ and the corresponding SNR in Table 3 along with the retrieval requirements.

The feasibility analysis is based upon three scenarios corresponding to the minimal, average and maximal expected spectral radiance levels according to Table 1. Equation 8 was solved for $\rho_{550nm}^{sfc} = 0.0, 0.3$ and 1.0 . to find the modeled L_{550nm}^{sensor} . The SNR requirements for aerosol retrieval were interpreted from the data, which are shown in Figure 2, where the SNR meets the requirement of $\varepsilon = 0.01$ (Equation 9).

The comparison in Table 3 between the retrieval requirement and the SNR of APEX reveals clearly the feasibility of aerosol retrieval for the analysed cases. However, it might be possible that the SNR does not meet the requirements for aerosol retrieval over the critical surface reflectance around $\rho_{550nm}^{sfc} = 0.5$ without additional binning.

Table 3. Feasibility analysis of the aerosol retrieval with APEX by comparing SNR values at $550nm$.

Radiance Level	Retrieval Requirement [SNR]	APEX Performance [SNR]	Feasibility
Minimum	$55 \left(\rho_{550nm}^{sfc} = 0.0 \right)$	86	OK
Average	$250 \left(\rho_{550nm}^{sfc} = 0.3 \right)$	325	OK
Maximum	$350 \left(\rho_{550nm}^{sfc} = 1.0 \right)$	862	OK

6. Summary and Conclusions

A spectral radiance simulation at the sensor level has been presented. It is capable of reproducing MODTRAN4 results under the SSA and within typical airborne remote sensing conditions. The multiple scattered path radiance was taken into account by the DISORT code [12]. This L_{λ}^{sensor} simulation was used to evaluate the noise equivalent difference aerosol optical thickness $NE \Delta \tau_{\lambda}^{aer}$ as a function of τ_{λ}^{aer} for different SNR and surface reflectances at $550nm$. The results reveal the sensor performance requirements for a sufficiently accurate AOD retrieval along with a feasibility analysis regarding APEX.

It has been shown that the detection of aerosols is feasible with APEX for low, average and high spectral radiance levels under the evaluated conditions (ie. solar, viewing and sensor configuration). This finding concerns the sensitivity requirements for an optical remote sensing instrument, such as APEX. The resulting feasibility is based on preflight sensor performance values; the final APEX SNR will be available after full scale calibration during the year 2008. Further investigations will be performed to assess the sensitivity and the limitations of the radiation transfer calculation and the aerosol retrieval algorithm itself.

We found that the spectral SNR is vital for aerosol remote sensing and varies strongly with surface reflectance. The latter strongly influences the intensity of L_{λ}^{sensor} , which drives the SNR. It has been shown that dark surfaces ($\rho_{550nm}^{sfc} < 0.1$) have the lowest SNR demands for aerosol retrieval. This is crucial for establishing feasibility because the sensor provides a lower SNR over dark surfaces due to the lower spectral radiance. The analysis showed that APEX is expected to provide sufficiently high SNR values even for black surfaces under the given conditions. More critical are relatively bright surfaces ($0.4 < \rho_{550nm}^{sfc} < 0.6$) because L_{550nm}^{sensor} depends only weakly on τ_{550nm}^{aer} . Extremely bright surfaces require again a lower SNR, but the unmixing of $L_{\lambda}^{atm} + L_{\lambda}^{sfc}$ is expected to be more difficult because of errors in the estimation of ρ_{λ}^{sfc} become dominant. Due to the small GSD of airborne instruments, it is expected that the identification of pure surface materials could be done with an adequate precision compared to satellite platforms. This allows to reduce the uncertainties in allocating a best-guess ρ_{λ}^{sfc} to the observed pixels and therefore alleviate the challenge of the unmixing of L_{λ}^{atm} from L_{λ}^{sensor} .

The finding of indefinitely high SNR requirements might be an artifact of the approximate simulation of L_{550nm}^{sensor} (Equation 8) for $\rho_{550nm}^{sfc} = 0.5 \pm 0.05$. It depends strongly upon the aerosol model assumption, in particular the approximation of the phase function and the multiple scattering. Further investigations are needed.

Generally, it was shown that an SNR of 300 or better will provide satisfying aerosol retrieval results for most surface reflectances considered in this analysis. Restricting the ranges to $\tau_{550nm}^{aer} < 0.25$ and $\rho_{550nm}^{sfc} < 0.2$, which are optimal and representative remote sensing conditions, an SNR of 100 is adequate. This is a promising finding in scope of the development of aerosol retrieval methods because most current instruments fulfill such SNR requirements under typical conditions.

Acknowledgments

We would like to acknowledge Dr. Alexander Kokhanovsky for sharing his expertise in the field of radiative transfer and multiple light scattering. We would also like to thank Jason Brazile and all involved individuals for their assistance. As well, we acknowledge the detailed and fruitful comments and suggestions of four anonymous reviewers.

References

1. King, M.; Kaufman, Y.; Tanré, D.; Nakajima, T. Remote sensing of tropospheric aerosols from space: Past, present, and future. *Bulletin of the American Meteorological Society* **1999**, *80*(11), 2229–2259.

2. Kokhanovsky, A. A.; Breon, F.-M.; Cacciari, A.; Carboni, E.; Diner, D.; Nicolantonio, W. D.; Grainger, R. G.; Grey, W. M. F.; Höller, R.; Lee, K.-H.; Li, Z.; North, P. R. J.; Sayer, A. M.; Thomas, G. E.; von Hoyningen-Huene, W. Aerosol remote sensing over land: a comparison of satellite retrievals using different algorithms and instruments. *Atmospheric Research* **2007**, *85*, 372–394.
3. Myhre, G.; Stordal, F.; Johnsrud, M.; Ignatov, A.; Mischenko, M. I.; Geogdzhayev, I. V.; Tanré, D.; Deuzé, J.-L.; Goloub, P.; Nakajima, T.; Higurashi, A.; Torres, O.; Holben, B. Intercomparison of satellite retrieved aerosol optical depth over the ocean. *Journal of Atmospheric Sciences* **2004**, *61*, 499–513.
4. Mishchenko, M. I.; Geogdzhayev, I. V.; Cairns, B.; Carlson, B. E.; Chowdhary, J.; Lacis, A. A.; Liu, L.; Rossow, W. B.; Travis, L. D. Past, present, and future of global aerosol climatologies derived from satellite observations: A perspective. *Journal of Quantitative Spectroscopy and Radiative Transfer* **2007**, *106*(1-3), 325–347.
5. Kahn, R. A.; Garay, M. J.; Nelson, D. L.; Yau, K. K.; Bull, M. A.; Gaitley, B. J.; Martonchik, J. V.; Levy, R. C. Satellite-derived aerosol optical depth over dark water from misr and modis: Comparisons with aeronet and implications for climatological studies. *Journal of Geophysical Research* **2007**, *112*(D18205).
6. Nieke, J.; Itten, K.; Debruyn, W. The airborne imaging spectrometer apex: from concept to realization. In *4th EARSeL Workshop on Imaging Spectroscopy*, **2005**.
7. Seidel, F.; Nieke, J.; Schläpfer, D.; Höller, R.; Hoyningen-Huene, W.; Itten, K. Aerosol retrieval for apex airborne imaging spectrometer: a preliminary analysis. In *Proc. of SPIE: Remote Sensing of Clouds and the Atmosphere X*, volume 5979, pages 548–557, **2005**.
8. Seidel, F.; Nieke, J.; Schläpfer, D.; Itten, K.; Bowles, J. Evaluation of near-uv/blue aerosol optical thickness retrieval from airborne hyperspectral imagery. In *Proc. IEEE-IGARSS, Denver, Colorado.*, pages 2247–2250, **2006**.
9. Schaepman, M.; Schläpfer, D.; Müller, A. Performance requirements for airborne imaging spectrometers. In *Proc. of SPIE: Imaging Spectrometry VII*, volume 4480, pages 23–31, **2002**.
10. Chandrasekhar, S. *Radiative Transfer*. Dover, New York, USA, **1960**. 393 pp.
11. Rozanov, V. V.; Kokhanovsky, A. A. The solution of the vector radiative transfer equation using the discrete ordinates technique: Selected applications. *Atmospheric Research* **2006**, *79*(3-4), 241–265.
12. Stamnes, K.; Tsay, S.-C.; Wiscombe, W.; Jayaweera, K. Numerically stable algorithm for discrete-ordinate-method radiative transfer in multiple scattering and emitting layered media. *Applied Optics* **1988**, *27*(12), 2502.
13. Berk, A.; Bernstein, L.; Robertson, D. MODTRAN: a moderate resolution model for LOW-TRAN7. Technical Report GL-TR-89-0122, Air Force Geophysics Lab, Hanscom AFB, Massachusetts, USA, **1989**.
14. Kokhanovsky, A. A.; Mayer, B.; Rozanov, V. V. A parameterization of the diffuse transmittance and reflectance for aerosol remote sensing problems. *Atmospheric Research* **2005**, *73*(1-2), 37–43.
15. Tanré, D.; Herman, M.; Deschamps, P. Y.; de Leffe, A. Atmospheric modeling for space measurements of ground reflectances, including bidirectional properties. *Applied Optics* **1979**, *18*(21), 3587.

16. Tanré, D.; Herman, M.; Deschamps, P. Influence of the background contribution upon space measurements of ground reflectance. *Applied Optics* **1981**, *20*(20), 3676–3684.
17. Vermote, E. F.; Tanré, D.; Deuzé, J. L.; Herman, M.; Morcrette, J.-J. Second simulation of the satellite signal in the solar spectrum, 6s: An overview. *IEEE Transactions on Geoscience and Remote Sensing*(May 1997), *35*(3), 675 – 686.
18. d’Almeida, G.; Koepke, P.; Shettle, E. *Atmospheric Aerosols: Global Climatology and Radiative Characteristics*. Deepak, Hampton, Virginia, USA, **1991**. 561 pp.
19. Bodhaine, B. A.; Wood, N. B.; Dutton, E. G.; Slusser, J. R. On rayleigh optical depth calculations. *Journal of Atmospheric and Oceanic Technology* **1999**, *16*(11), 1854–1861.
20. Richter, R.; Schläpfer, D. Geo-atmospheric processing of airborne imaging spectrometry data. Part 2: atmospheric/topographic correction. *International Journal of Remote Sensing* **2002**, *23*(13), 2631–2649.
21. Schläpfer, D.; Schaepman, M. Modeling the noise equivalent radiance requirements of imaging spectrometers based on scientific applications. *Applied Optics* **2002**, *41*(27), 5691–5701.